

TECHNICAL RESEARCH REPORT

Isotropic Design of Tendon-Driven Manipulators

by Y-J. Ou, L-W. Tsai

T.R. 95-95



*Sponsored by
the National Science Foundation
Engineering Research Center Program,
the University of Maryland,
Harvard University,
and Industry*

Isotropic Design of Tendon-Driven Manipulators

Yeong-Jeong Ou
Graduate Research Assistant

Lung-Wen Tsai
Professor
Fellow ASME

Mechanical Engineering Department
and
Institute for Systems Research
The University of Maryland
College Park, Maryland

ABSTRACT

This paper deals with the synthesis of mechanical transmission structures for tendon-driven manipulators. Based on static force analysis, necessary conditions are developed for the synthesis of tendon-driven manipulators with isotropic transmission characteristics. It is shown that an n degree-of-freedom (dof) manipulator will possess the isotropic transmission characteristics, if it satisfies two isotropic conditions. Furthermore, a design equation is derived for the construction of isotropic transmission structure matrices and a three-dof spatial manipulator is synthesized to demonstrate the methodology. It is shown that the isotropic design leads to a more uniform tendon force distribution.

1 Introduction

Various transmission mechanisms such as gear trains, bar linkages and tendon drives (cables, timing belts, chains, etc.) can be utilized for transmitting force and/or torque from actuators to the joints of a manipulator. The choice of a transmission mechanism depends on the application and other design considerations. In general, load capacity to weight ratio should be maximized, backlash and compliance problems minimized, and friction reduced. Among the various transmission mechanisms, tendon drives offer the features of light weight, compact size, and little backlash. These merits have made tendons better suited than other transmission mechanisms in applications such as dexterous hands where the requirements of small volume, light weight, and high speed are of fundamental concern.

Tendon drives can generally be classified into two groups: *endless tendon drives* and *open-ended tendon drives*. In an endless tendon drive, each tendon wraps around several pulleys in a closed loop to drive a system. Endless tendon drives can be concatenated in series to form a multi-stage transmission system similar to a gear train (Salisbury, 1987; Lee and Tsai, 1989; Townsend and Salisbury, 1991). Force transmission in an endless tendon drive usually relies on friction generated between pulleys and belts. To prevent belts from slipping, toothed belts known as the *timing belts* or *chain-and-sprockets* can be employed. In an endless tendon transmission system, one-half of the belt will be under high tension while the other half subjects to little tension. Although force transmission can be bi-directional, pretension of the belts is necessary to prevent belts from slacking. To overcome the above difficulty, open-ended tendon drives may be used. In an open-ended tendon transmission system, one end of a tendon is attached to a moving link while the other end is pulled by an actuator and force is transmitted by pulling of the tendons.

A unique feature associated with tendon drives is that tendons can only exert tension but not compression. Because of this special characteristic, Merecki et al. (1980) pointed out that an n degree-of-freedom (dof) manipulator requires at least $n+1$ open-ended tendons to gain a full control of the manipulator. For examples, each three-dof finger in the Stanford/JPL hand is controlled by four tendons (Salisbury, 1982), and each four-dof finger in the Utah/MIT hand is controlled by eight tendons (Jacobsen et al., 1984 and 1986). When the number of tendons m is less than $n+1$, the manipulation must rely on mechanical constraints and/or other kinematical and dynamical characteristics. For example, Hirose and Umetani (1978 and 1979) designed a soft gripper in which each multi-dof finger is controlled by just one grip tendon and one release tendon. Recently, Albus et al. (1992) developed a robotic crane system in which six cables are used as parallel links to manipulate the position and orientation of a suspended platform. Although the number of tendons (and

actuators) m is less than $n + 1$, full control of the end-effector is possible due to the fact that the gravitational force is employed as the $(n + 1)^{th}$ control force.

Numerous open-ended tendon-driven manipulators have been designed. Morecki et al (1980) designed an anthropomorphic two-handed manipulator. Salisbury et al. (1988) design a whole-arm manipulator. Hirose and Shugen (1991) designed a “CT” arm. We note that most tendon-driven manipulators are designed to minimize tendon forces needed to overcome the gravity. For space applications and dexterous hands where the links are light and the effects of gravitational force can be neglected, other kinematic properties such as isotropic force transmission may become more important design factors.

Salisbury (1982) performed the transmission error of the Stanford/JPL hand and defined those end-effector positions where the condition number of the Jacobian matrix is equal to one as the isotropic points. Asada and Cro Granito (1985) used the generalized velocity ratios and the mobility ellipsoid as a measure of the kinematic performance. When the maximal generalized velocity ratio is equal to the minimal ratio, the manipulator is said to possess an isotropic mobility. Gosselin and Angeles (1988) defined an index based on the condition number of the Jacobian matrix for kinematic optimization of manipulators.

The aforementioned condition number is defined as the ratio of the maximal singular value to the minimal singular value of the Jacobian matrix. The Jacobian matrix relates the static force transmission between the joint space and the end-effector space. It does not consider the effect of force and/or torque transmission between the actuators and the joints. To overcome this shortcoming, Lee and Tsai (1991) studied the force transmission between the tendon space and the joint space. Subsequently, Chen and Tsai (1993) considered the overall force transmission from the actuator space to the end-effector space and derived an isotropic transmission condition for the synthesis of geared robotic mechanisms. However, Chen and Tsai’s results are not directly applicable to tendon-driven manipulators. In this paper, we shall consider the overall force transmission and derive the necessary conditions to arrive at an isotropic design of a tendon-driven manipulator. We shall limit ourselves to a class of open-ended tendon-driven manipulators for which the number of tendons is at least equal to $n + 1$ and not more than $2n$.

2 Static Force Transmission

Figure 1 shows the planar schematic of an n -dof spatial manipulator with m control tendons. Note that for the convenience of matrix operation, we have numbered the

links and joints sequentially from the distal end. Neglecting the gravitational force and applying the principle of virtual work, the transformation between the joint torques and the tendon forces can be derived as (Lee and Tsai, 1989):

$$\boldsymbol{\tau} = \mathbf{B} \underline{\xi} \quad (1)$$

where $\boldsymbol{\tau}$ is an n -dimensional joint torque vector, $\underline{\xi}$ is an m -dimensional tendon force vector, and \mathbf{B} is an $n \times m$ matrix called the *structure matrix*.

In general, the structure matrix \mathbf{B} is a function of tendon routing, pulley sizes, and end-effector position. In what follows, we shall assume that tendons are routed from the joint to joint over circular pulleys in a continuous manner. This way, \mathbf{B} is independent of the end-effector position. Furthermore, the non-zero elements in each column of \mathbf{B} are consecutive.

Given a desired joint torque vector $\boldsymbol{\tau}$, Eq. (1) represents n linear equations in m unknown tendon forces. Hence, to achieve independent control of the joint torques, \mathbf{B} should be a full-rank matrix and, with $m > n$, the pseudo-inverse transformation can be written as (Ben-Israel and Greville, 1974):

$$\underline{\xi} = \mathbf{B}^+ \boldsymbol{\tau} + \mathbf{H} \underline{\lambda} \quad (2)$$

where $\mathbf{B}^+ = \mathbf{B}^T[\mathbf{B}\mathbf{B}^T]^{-1}$ is the pseudo-inverse of \mathbf{B} , \mathbf{H} is an $m \times (m - n)$ matrix with its column vectors spanning the null space of \mathbf{B} , and $\underline{\lambda}$ is an arbitrary $(m - n)$ -dimensional vector.

The first term in the right-hand side of eq. (2) is known as the *particular solution* and the second term the *homogeneous solution*. Assuming a positive value of ξ_i ($i = 1, 2, 3, \dots, m$) represents tension and a negative value represents compression, then all the elements of $\underline{\xi}$ in eq. (2) should be kept non-negative. In this regard, we conclude that the column space of \mathbf{H} should contain at least one m -dimensional vector with all positive elements such that non-negative tendon forces can be maintained by adjusting the vector $\underline{\lambda}$. Based on the above assumptions and discussions, we conclude that the structure matrix should satisfy the following characteristics:

- C1. The rank of \mathbf{B} is equal to n .
- C2. There exists at least one vector with all positive elements in the null space of \mathbf{B} .

C3. Non-zero elements in each column of \mathbf{B} are consecutive.

Neglecting the gravitational force and applying the principle of virtual work, it can be shown that the joint torque vector is related to the end-effector force vector by (Salisbury and Craig, 1982):

$$\underline{\tau} = \mathbf{J}^T \underline{f} \quad (3)$$

where \underline{f} is an n -dimensional end-effector force vector, and \mathbf{J} is an $n \times n$ Jacobian matrix. Note that the end-effector force vector may contain both force and moment vectors. In what follows, we shall limit ourselves to manipulators whose tasks are of one single type, namely, either point-positioning or body-orientation, but not both. This way, the elements of the Jacobian matrix will have uniform dimensions.

Substituting eq. (3) into (2), yields

$$\underline{\xi} = \mathbf{B}^+ \mathbf{J}^T \underline{f} + \mathbf{H} \underline{\lambda} \quad (4)$$

The particular solution in eq. (4) is the minimum norm solution which might contain negative tendon forces. However, by adjusting the vector $\underline{\lambda}$, the homogeneous solution can be amplified to compensate for these negative forces such that the resulting tendon forces become non-negative. Thus, both the particular solution and the homogeneous solution have significant effects on tendon forces. That is, the structure matrix \mathbf{B} and the Jacobian matrix \mathbf{J} are equally important to the force transmission of a tendon-driven manipulator.

3 Isotropic Transmission Conditions

For a tendon-driven manipulator, the feasible domain of tendon forces spans only the positive hyperquadrant of an m -dimensional space. It can be seen from eq. (4) that the particular solution is obtained as a linear transformation of the end-effector force \underline{f} . In general, a unit hypersphere in the n -dimensional end-effector force space maps into an n -dimensional ellipsoid in the m -dimensional tendon force space. The space occupied by this n -dimensional ellipsoid is called the particular solution subspace. A superposition of the particular solution with the homogeneous solution translates the n -dimensional ellipsoid into the positive hyperquadrant of the m -dimensional tendon

force space, by adjusting $\underline{\lambda}$. Therefore, an isotropic transmission structure can be characterized by the following two conditions.

3.1 Condition 1

The condition number of a matrix gives an indication of the error sensitivity in a linear transformation system (Strang, 1980). Here, we require the condition number of $\mathbf{B}^+\mathbf{J}^T$ to be equal to one such that a unit hypersphere in the end-effector force space maps into a hypersphere in the particular solution subspace, and the mapping is scaled isometrically. This leads to

$$\mathbf{J}(\mathbf{B}^+)^T\mathbf{B}^+\mathbf{J}^T = \mu^2 \mathbf{I}_n \quad (5)$$

where μ is the multiple singular value of $\mathbf{B}^+\mathbf{J}^T$ and \mathbf{I}_n is the n -dimensional identity matrix.

Applying the definition of pseudo-inverse, eq. (5) can be simplified as

$$\mathbf{J}(\mathbf{B}\mathbf{B}^T)^{-1}\mathbf{J}^T = \mu^2 \mathbf{I}_n \quad (6)$$

Pre-multiplying \mathbf{J}^{-1} and post-multiplying $(\mathbf{J}^T)^{-1}$ to both sides of eq. (6), yields

$$\mathbf{B}\mathbf{B}^T = \frac{1}{\mu^2}(\mathbf{J}^T\mathbf{J}) \quad (7)$$

Equation (7) is valid at those end-effector positions where the Jacobian matrix is non-singular.

3.2 Condition 2

With both origins of the n -dimensional particular solution subspace and the m -dimensional tendon force space coinciding, the orthogonally projected vectors of the positive Cartesian axes of the m -dimensional tendon force space should be evenly spaced in the n -dimensional particular solution subspace.

It is well known that an n -dimensional regular convex polytope can be formed by connecting the apexes of m evenly spaced vectors of equal lengths. In the 2-D space, a regular m -polygon can be formed by connecting the apexes of any $m \geq 3$ evenly spaced vectors of equal lengths. In the 3-D space, there exists only five regular polyhedrons (the five Platonic solids). In the n -D space, a regular polytope contains $n + 1$, $2n$, or $2^n, \dots$, apexes (Coxeter, 1973).

Since each apex represents a tendon or an actuator, kinematic isotropy is feasible only for manipulators designed with certain number of tendons. For 2-dof manipulators, any $m \geq 3$ number of tendons can be routed to possess isotropic transmission characteristics. For $n > 2$ dof manipulators, the feasible number of tendons are $n + 1$, $2n$, 2^n , etc. When m is larger than $2n$, tendon routing will be too complex to be practical. In what follows, we shall consider manipulators with $n + 1$ and $2n$ tendons.

In the n -dimensional space, a regular simplex polytope has $n + 1$ apexes and the angle subtended by each edge at the center of the polytope is equal to $\cos^{-1}(-1/n)$. Let the origin of a Cartesian frame be located at the center of the regular simplex; the coordinates of each apex be denoted by a column vector; and the distance from the origin to each apex be equal to one unit length. Then, the coordinates of the apexes can be expressed by an $n \times (n + 1)$ pseudo-triangular matrix as given below:

$$\tilde{\mathbf{P}}_{n+1} = \sqrt{\frac{n+1}{2n}} \begin{bmatrix} 1 & -1 & 0 & 0 & 0 & \dots & 0 \\ 1/\sqrt{3} & 1/\sqrt{3} & -2/\sqrt{3} & 0 & 0 & \dots & 0 \\ 1/\sqrt{6} & 1/\sqrt{6} & 1/\sqrt{6} & -3/\sqrt{6} & 0 & \dots & 0 \\ \vdots & \vdots & \vdots & \vdots & \vdots & \dots & \vdots \\ \sqrt{\frac{2}{n^2+n}} & \sqrt{\frac{2}{n^2+n}} & \cdot & \cdot & \cdot & \dots & -\sqrt{\frac{2n^2}{n^2+n}} \end{bmatrix} \quad (8)$$

The null space of $\tilde{\mathbf{P}}_{n+1}$ is an $(n + 1)$ -dimensional vector given by:

$$\tilde{\mathbf{H}}_{n+1} = [1, 1, 1, \dots, 1]^T \quad (9)$$

We called the vector $\tilde{\mathbf{H}}_{n+1}$ the *isotropic vector*.

A regular cross polytope has $2n$ apexes, and the angle subtended by each edge at the center of the polytope is equal to 90° . Let the coordinates of each apex be represented by a column vector. Then, with the center of the polytope located at the origin of a Cartesian frame and the distance from the origin to each apex be equal to one unit length, the coordinates of the $2n$ apexes can be expressed by an $n \times 2n$ matrix as given below:

$$\tilde{\mathbf{P}}_{2n} = \begin{bmatrix} 1 & -1 & 0 & 0 & 0 & \cdots & 0 & 0 \\ 0 & 0 & 1 & -1 & 0 & \cdots & 0 & 0 \\ \vdots & \vdots & \vdots & \vdots & \vdots & \cdots & \vdots & \vdots \\ 0 & 0 & 0 & 0 & 0 & \cdots & 1 & -1 \end{bmatrix} \quad (10)$$

Note that $\tilde{\mathbf{P}}_{2n}$ contains two opposing column vectors (apexes) located on each axis of the n -dimensional Cartesian space, and the inner product of any two column vectors is equal to zero or minus one.

The null space of matrix $\tilde{\mathbf{P}}_{2n}$ is a $2n \times n$ matrix given by:

$$\tilde{\mathbf{H}}_{2n} = \begin{bmatrix} 1 & 0 & \cdots & 0 \\ 1 & 0 & \cdots & 0 \\ 0 & 1 & \cdots & 0 \\ 0 & 1 & \cdots & 0 \\ \vdots & \vdots & \cdots & \vdots \\ 0 & 0 & \cdots & 1 \\ 0 & 0 & \cdots & 1 \end{bmatrix} \quad (11)$$

Although the null space of a matrix obtained by exchanging any two columns of $\tilde{\mathbf{P}}_{2n}$ is different from that of the matrix $\tilde{\mathbf{P}}_{2n}$ itself, they represent a permutation of the order of the apexes and, hence, are isomorphic to one another.

By rotating a regular polytope with respect to the Cartesian frame, the matrices shown in eqs. (8) and (10) can be transformed into the following form:

$$\mathbf{P}_m = \mathbf{U}\tilde{\mathbf{P}}_m \quad (12)$$

where $m = n + 1$ or $2n$, and \mathbf{U} is an $n \times n$ rotation matrix. Since the row vectors of \mathbf{P}_m are orthogonal to each other, we have

$$\mathbf{P}_m \mathbf{P}_m^T = \alpha_m^2 \mathbf{I}_n \quad (13)$$

where $\alpha_{n+1} = \sqrt{(n+1)/n}$ and $\alpha_{2n} = \sqrt{2}$.

Since the complementary space of the column space of $\tilde{\mathbf{H}}_m$ ($m = n + 1$ or $2n$) is

the row space of \mathbf{P}_m , any matrix with the null space of the form of eq. (9) or (11) spans the same space as \mathbf{P}_m and, therefore, possesses the characteristic of projecting orthogonally the m -dimensional Cartesian axes uniformly in the n -dimensional particular solution subspace. Therefore, an isotropic transmission structure should satisfy

$$\mathbf{B}\tilde{\mathbf{H}}_m = 0, \quad \text{for } m = n + 1 \text{ or } 2n \quad (14)$$

Equation (14) states that the null space of \mathbf{B} is given by Eq. (9) or (11).

From the above derivations, we conclude that an n -dof tendon-driven manipulator can be designed to possess the isotropic transmission characteristics at a designated position, if it is constructed with either $n + 1$ or $2n$ tendons, and if its structure matrix \mathbf{B} and Jacobian matrix \mathbf{J} satisfy eqs. (7) and (14).

4 Design Equation

In what follows, we apply eqs. (7) and (14) to derive a design equation for the construction of a structure matrix with the isotropic transmission characteristics. First, we apply the “skinny” QR factorization to the matrices \mathbf{B}^T and J (Golub and Van Loan, 1989), i.e.,

$$\mathbf{B}^T = \mathbf{Q}_1 \mathbf{R}_1 \quad (15)$$

and

$$\mathbf{J} = \mathbf{Q} \mathbf{R} \quad (16)$$

where \mathbf{Q}_1 is an $m \times n$ matrix with orthonormal columns, \mathbf{R}_1 is an $n \times n$ upper triangular matrix with positive diagonal entries, \mathbf{Q} is an $n \times n$ orthonormal matrix, and \mathbf{R} is an $n \times n$ upper triangular matrix. Note that J must be a full rank matrix at a prescribed end-effector position.

Substituting eqs. (15) and (16) into (7), and using the fact that

$$\mathbf{Q}_1^T \mathbf{Q}_1 = \mathbf{Q}^T \mathbf{Q} = \mathbf{I}_n \quad (17)$$

we obtain

$$\mathbf{R}_1^T \mathbf{R}_1 = \frac{1}{\mu^2} \mathbf{R}^T \mathbf{R} \quad (18)$$

Since both sides of eq. (18) are in the form of Cholesky factorization, we conclude that

$$\mathbf{R}_1 = \frac{1}{\mu} \mathbf{R} \quad (19)$$

Substituting the transpose of eq. (15) into (14), yields

$$\mathbf{R}_1^T \mathbf{Q}_1^T \tilde{\mathbf{H}}_m = \mathbf{0} \quad (20)$$

Since \mathbf{R}_1^T is a full-rank matrix, its null space is empty. Hence, eq. (20) reduces to

$$\mathbf{Q}_1^T \tilde{\mathbf{H}}_m = \mathbf{0} \quad (21)$$

From eqs. (17) and (21), it can be shown that

$$\mathbf{Q}_1^T = \frac{1}{\alpha_m} \mathbf{P}_m \quad (22)$$

Substituting eqs. (19) and (22) into the transpose of eq. (15), yields

$$\mathbf{B} = c_m \mathbf{R}^T \mathbf{P}_m = c_m \mathbf{R}^T \mathbf{U} \tilde{\mathbf{P}}_m \quad (23)$$

where $c_m = 1/(\mu\alpha_m)$. Using eq. (23), isotropic transmission structure matrix can be synthesized.

5 Discussions

If the isotropic point is chosen at a position where the condition number of \mathbf{J} is equal to one and \mathbf{U} is an identity matrix, then the structure matrix is given by $\tilde{\mathbf{P}}_{n+1}^T$ or $\tilde{\mathbf{P}}_{2n}$. Since $\tilde{\mathbf{P}}_{n+1}^T$ is already in a pseudotriangular form, it permits all actuators to be base mounted. However, since $\tilde{\mathbf{P}}_{2n}$ is a bi-diagonal matrix, it does not permit all actuators to be base mounted.

Each column of the structure matrix represents a mechanical transmission line contributed by one tendon. Corresponding to each transmission line in an isotropic structure matrix \mathbf{B}_{2n} , there exists an opposing transmission line. We call these two opposing transmission lines a *dual transmission line*. Thus, the simplest isotropic transmission structure with base mounted actuators takes the following form:

$$\mathbf{B}_{2n} = \begin{bmatrix} a_1 & -a_1 & 0 & 0 & \cdots & 0 & 0 \\ a_2 & -a_2 & b_2 & -b_2 & \cdots & 0 & 0 \\ \vdots & \vdots & \vdots & \vdots & \vdots & \vdots & \vdots \\ a_{n-1} & -a_{n-1} & b_{n-1} & -b_{n-1} & \cdots & 0 & 0 \\ a_n & -a_n & b_n & -b_n & \cdots & e_n & -e_n \end{bmatrix} \quad (24)$$

A matrix of the above form is called an $n \times 2n$ *pseudo-triangular matrix*. In general, unless \mathbf{U} is an identity matrix, \mathbf{P}_m will contain non-zero elements in the upper-right and lower-left corners of the matrix. Since the matrix \mathbf{R} in eq. (23) is an upper triangular matrix, we conclude that for \mathbf{B}_{2n} to be a pseudo-triangular matrix, \mathbf{U} must be an identity matrix and all elements in the upper triangle of \mathbf{R} must be non-zero. This implies that whether a pseudo-triangular structure matrix can be achieved or not depends on the matrix \mathbf{R} , i.e., the link geometry and the choice of the end-effector position. This also implies that a pseudo-triangular isotropic structure matrix cannot be achieved at the position where the condition number of \mathbf{J} is equal to one.

6 Example

Transmission structures with $n + 1$ tendons have been investigated previously by Ou and Tsai (1993). In this paper, we shall concentrate ourselves on those transmission structures with $2n$ tendons. The isotropic design of a 3-dof spatial manipulator will be examined to illustrate the methodology.

Figure 2 shows a three-dof spatial manipulator in which the middle and distal joint axes are parallel to one another and are both perpendicular to the base joint axis. The lengths of the distal and proximal links are both equal to $1/\sqrt{2}$ times that of the middle link.

The Jacobian matrix of the manipulator expressed in the link OA coordinate system can be written as

$$\mathbf{J} = \ell \begin{bmatrix} 0 & 0 & -C_2 - (1 + C_{12})/\sqrt{2} \\ -S_{12}/\sqrt{2} & -S_2 - S_{12}/\sqrt{2} & 0 \\ C_{12}/\sqrt{2} & C_2 + C_{12}/\sqrt{2} & 0 \end{bmatrix} \quad (25)$$

where ℓ is the length of the middle link, $C_2 = \cos(\theta_2)$, $S_2 = \sin(\theta_2)$, $C_{12} = \cos(\theta_1 + \theta_2)$, and $S_{12} = \sin(\theta_1 + \theta_2)$. In what follows, we let $\ell = 1$ unit length. For this manipulator, the condition number of the Jacobian matrix is equal to one when $\theta_1 = 135^\circ$ and $\theta_2 = 45^\circ$, and the $x = 0$ and $y = z = 1/\sqrt{2}$ is one such point on the locus.

The matrix \mathbf{R} from the QR factorization of the Jacobian matrix contains zero elements in the upper-triangle. Hence, an isotropic structure matrix of the pseudo-triangular form is infeasible. In what follows, we seek for a non-pseudo-triangular tendon routing.

Two transmission structures as shown in Table 1 are synthesized for the purpose of comparison. Structure (a) is designed with equal size pulleys. Structure (b) is derived from eq. (23) using the following rotation matrix:

$$\mathbf{U} = \begin{bmatrix} 1 & 0 & 0 \\ 0 & \cos(3\pi/4) & \sin(3\pi/4) \\ 0 & -\sin(3\pi/4) & \cos(3\pi/4) \end{bmatrix} \begin{bmatrix} \cos(-\pi/4) & \sin(-\pi/4) & 0 \\ -\sin(-\pi/4) & \cos(-\pi/4) & 0 \\ 0 & 0 & 1 \end{bmatrix} \quad (26)$$

Structure (a) does not possess the isotropic transmission characteristics within its workspace, and structure (b) possesses the isotropic transmission characteristics at the $x = 0$ and $y = z = 1/\sqrt{2}$ position. The tendon routings are shown in Fig. 3. The variable κ shown in Table 1 is a scaling factor for sizing the pulleys. To achieve a fair comparison, the values of κ are determined from the condition that the product of the three singular values of \mathbf{B} is equal to one. Table 1 also shows the homogeneous solutions of these two structure matrices.

Two positions are chosen for the evaluation. Position 1 is chosen at $x = 0$ and $y = z = 1/\sqrt{2}$ which is the isotropic position for structure (b), and position 2 is

chosen at $x = 0, y = 1 + 1/\sqrt{2}$, and $z = 0$. Let a unit force \underline{f}^* be applied at the end-effector as shown in Fig. 2. As the applied force changes its direction, tendon forces are computed by using eq. (4). In computing the tendon forces, the vector $\underline{\lambda}$ is adjusted such that the smallest tendon force is equal to zero.

Figures 4 and 5 show the spherical plots of tendon forces for the two transmission structures evaluated at position 1. In a spherical plot, the radial distance represents the magnitude of a tendon force, and the direction represents the direction of applied force. Since the routings of tendons 1, 3, and 5 are opposite to that of tendons 2, 4, and 6, respectively, only three of the six tendon forces are plotted in Figs. 4 and 5. We note that each tendon experiences zero force over one-half of the end-effector force space. Since position 1 is an isotropic position for structure (b), the spherical plots of tendon forces shown in Fig. 5 are identical in shape and size except for a shift in the phase angle. Since structure (a) does not possess the isotropic transmission characteristics, the spherical plots of tendon forces shown in Fig. 4 are different from each other.

Table 2 lists the maximum tensions, their ratios, and the condition numbers of $\mathbf{B}^+\mathbf{J}^T$ for the manipulator evaluated at the two prescribed positions. Although both transmission structure matrices share the same homogeneous solution, the condition number of structure (b) is much better than that of structure (a) for both positions. At position 1, the ratios of the maximum tendon forces are equal to 1.0 : 1.0 : 1.0 : 1.0 : 1.0 : 1.0 for structure (b) and 1.0 : 1.0 : 1.4 : 1.4 : 1.4 : 1.4 for structure (a). As the end-effector moves to position 2, the ratios of the maximum tendon forces changed slightly for structure (b), but they become much worse for structure (a). We conclude that structure (b) has a more uniform tendon force distribution than structure (a).

7 Summary

Based on the static force analysis, necessary conditions for a tendon-driven manipulator to possess isotropic transmission characteristics are derived. Two isotropic transmission conditions are derived: (1) The condition number of the overall transformation matrix, $\mathbf{B}^+\mathbf{J}^T$, should be equal to one, and (2) the number of tendons m should be equal to $n+1$ or $2n$ (assuming that $m \leq 2n$) and the null space of the structure matrix is given by $\tilde{\mathbf{H}}_m$. Using these two conditions, a design equation is derived for the isotropic synthesis of tendon-driven manipulators. Furthermore, the isotropic design of a three-dof spatial manipulator is examined to demonstrate the methodology. It is shown that a manipulator with the isotropic transmission characteristics has more uniform force distribution among its tendons.

We note that the isotropic transmission characteristics only exist at a prescribed position. Therefore, careful consideration should be given to the selection of the isotropic position in order to achieve a near optimal kinematic performance within the entire workspace. According to our experience, a manipulator will generally possess nice transmission characteristics within its workspace, if the isotropic point is chosen around the mid-range of the workspace.

Finally, we point out that the isotropic transmission characteristics should not be over emphasized. For some applications, it may be advantageous to design a transmission mechanism with non-isotropic transmission characteristics and this can be achieved by multiplying a weighting matrix to the Jacobian matrix.

Acknowledgment

This work was supported in part by the U.S. Department of Energy under Grant DEF05-88ER13977, and in part by the NSF Engineering Research Centers Program NSFD CDR 8803012. Such support does not constitute an endorsement by the supporting agencies of the views expressed in the paper.

References

1. Albus, J., Bostelman, R., and Dagalakis, N., 1992, "The NIST Spider, A Robot Crane," *Journal of Research of the NIST*, Vol. 97, No. 3, pp. 373-385.
2. Asada, H., and Cro Granito, J.A., 1985, "Kinematic and Static Characterization of Wrist Joints and Their Optimal Design," *Proc. of IEEE 1985 Int'l Conf. on Robotics and Automation*, pp. 244-250.
3. Ben-Israel, A., and Greville, T.N.E., 1974, *Generalized Inverses: Theory and Applications*, Wiley, New York, N.Y.
4. Chen, D.Z., and Tsai, L.W., 1993, "Kinematic and Dynamic Synthesis of Geared Robotic Mechanisms," *ASME J. of Mechanical Design*, Vol. 115, No. 2, pp. 241-246.
5. Coxeter, H.S.M., 1973, *Regular Polytopes*, 3rd ed., Dover Publications, New York, N.Y.
6. Craig, J.J., 1986, *Introduction to Robotics*, Addison Wesley, Readings, Mass.
7. Golub, G.H., and Van Loan, C.F., 1989, *Matrix Computations*, 2nd ed., The John Hopkins University Press, Baltimore, MD.

8. Gosselin, C., and Angeles, J., 1988, "A New Performance Index for the Kinematic Optimization of Robotic Manipulators," *ASME Trends and Developments in Mechanisms, Machines and Robotics*, DE-Vol. 15-3, pp. 441-447.
9. Hirose S., and Umetani Y., 1978, "The Development of Soft Gripper for the Versatile Robot Hand," *Mechanism and Machine Theory*, Vol. 13, pp. 351-359.
10. Hirose, S., and Umetani, Y., 1979, "The Kinematics and Control of a Soft Gripper for the Handling of Living or Fragile Objects," *Proc. of the Fifth World Congress on the Theory of Machines and Mechanisms*, pp. 1175-1178.
11. Hirose, S., and Shugen, M., 1991, "Coupled Tendon-Driven Multijoint Manipulator," *Proc. IEEE Int'l Conf. on Robotics and Automation*, Vol. 2, pp. 1268-1275.
12. Jacobsen, S.C., Wood, J.E., Knutti, D.F., and Biggers, K.B., 1984, "The Utah/MIT Dexterous Hand: Work in Progress," *The Int'l J. of Robotics Research*, Vol. 3, No. 4, pp. 21-50.
13. Jacobsen, S.C., Iversen, E.K., Knutti, D.F., Johnson, R.T., and Biggers, K.B., 1986, "The Design of the Utah/MIT Dextrous Hand," *Proc. IEEE Int'l Conf. on Robotics and Automation*, pp. 1520-1532.
14. Lee, J.J., and Tsai, L.W., 1989, "Kinematic Analysis of Tendon-Driven Robotic Mechanisms Using Graph Theory," *ASME J. of Mechanisms, Transmissions, and Automation in Design*, Vol. 111, No. 1, pp. 59-65.
15. Lee, J.J., and Tsai, L.W., 1991, "Topological Analysis of Tendon-Driven Manipulators," *8th World Congress on Int'l Federation of the Theory of Machines and Mechanisms*, Czechoslovakia, pp. 479-482.
16. Morecki, A., Busko, Z., Gasztold, H., and Jaworek, K., 1980, "Synthesis and Control of the Anthropomorphic Two-Handed Manipulator," *Proc. 10th Int'l Symposium on Industrial Robots*, Milan, Italy, pp. 461-474.
17. Ou, Y.J., and Tsai, L.W., 1993, "Kinematic Synthesis of Tendon-Driven Manipulators with Isotropic Transmission Characteristics," *ASME J. of Mechanical Design*, Vol. 115, No. 4, pp. 884-891.
18. Salisbury, J.K., 1982, "Kinematic and Force Analysis of Articulated Hands," Ph.D. Dissertation, Mech. Eng. Dept., Stanford University, Stanford, CA.
19. Salisbury, J.K., and Craig, J.J., 1982, "Articulated Hands: Force Control and Kinematic Issues," *The Int'l J. of Robotics Research*, Vol. 1, No. 1, pp. 4-17.
20. Salisbury, J.K., 1987, "Whole-Arm Manipulation," *Proc. 4th Intl. Symposium on Robotics Research*, Santa Cruz, CA.

21. Salisbury, J.K., Townsend, W., Eberman, B., and Dipietro D., 1988, "Preliminary Design of A Whole-Arm Manipulation System (WAMS)," *Proc. of IEEE int'l Conf. on Robotics and Automation*, Vol. 1, pp. 254-260.
22. Strang, G., 1980, *Linear Algebra and Its Applications*, 2nd ed., Academic Press, New York, N.Y.
23. Townsend, W.T., and Salisbury, J.K., 1991, "Mechanical Bandwidth as a Guideline to High-Performance Manipulator Design," *Proc. IEEE Int'l Conf. on Robotics and Automation*, Vol. 3, pp. 1390-1395.

List of Tables

1. Two transmission structures and their kinematic properties.
2. List of maximum tensions, their ratios and the condition numbers.

List of Figures

1. Planar Schematic of an n -dof manipulator with m tendons (Note that the joints are sequentially numbered from the distal end).
2. A three-dof spatial manipulator.
3. Tendon routings for transmission structures (a) and (b).
4. Spherical plots of tendon forces versus direction of applied force for structure (a).
5. Spherical plots of tendon force versus direction of applied force for structure (b).

	B	κ	H
(a)	$\kappa \begin{bmatrix} 1 & -1 & 0 & 0 & 0 & 0 \\ 1 & -1 & 1 & -1 & 0 & 0 \\ 1 & -1 & 1 & -1 & 1 & -1 \end{bmatrix}$	0.707	$\begin{bmatrix} 1 & 0 & 0 \\ 1 & 0 & 0 \\ 0 & 1 & 0 \\ 0 & 1 & 0 \\ 0 & 0 & 1 \\ 0 & 0 & 1 \end{bmatrix}$
(b)	$\kappa \begin{bmatrix} 1 & -1 & 1 & -1 & 0 & 0 \\ \frac{1}{\sqrt{2}} & \frac{-1}{\sqrt{2}} & \frac{-1}{\sqrt{2}} & \frac{1}{\sqrt{2}} & 1 & -1 \\ \frac{1}{\sqrt{2}} & \frac{-1}{\sqrt{2}} & \frac{-1}{\sqrt{2}} & \frac{1}{\sqrt{2}} & -1 & 1 \end{bmatrix}$	0.500	$\begin{bmatrix} 1 & 0 & 0 \\ 1 & 0 & 0 \\ 0 & 1 & 0 \\ 0 & 1 & 0 \\ 0 & 0 & 1 \\ 0 & 0 & 1 \end{bmatrix}$

Table 1: Two transmission structures and their kinematic properties.

Structure		(a)	(b)
1	max. tension	$\begin{bmatrix} 1 \\ 1 \\ 1.414 \\ 1.414 \\ 1.414 \\ 1.414 \end{bmatrix}$	$\begin{bmatrix} 1 \\ 1 \\ 1 \\ 1 \\ 1 \\ 1 \end{bmatrix}$
	ratio	1 : 1 : 1.4 : 1.4 : 1.4 : 1.4	1 : 1 : 1 : 1 : 1 : 1
	Cond($\mathbf{B}^+\mathbf{J}^T$)	4.0489	1
2	max. tension	$\begin{bmatrix} 1 \\ 1 \\ 1.414 \\ 1.414 \\ 2.798 \\ 2.798 \end{bmatrix}$	$\begin{bmatrix} 1.677 \\ 1.677 \\ 1.450 \\ 1.450 \\ 1.978 \\ 1.978 \end{bmatrix}$
	ratio	1 : 1 : 1.4 : 1.4 : 2.8 : 2.8	1.2 : 1.2 : 1 : 1 : 1.4 : 1.4
	Cond($\mathbf{B}^+\mathbf{J}^T$)	3.6313	2.7112

Table 2: List of maximum tensions, their ratios and the condition numbers.

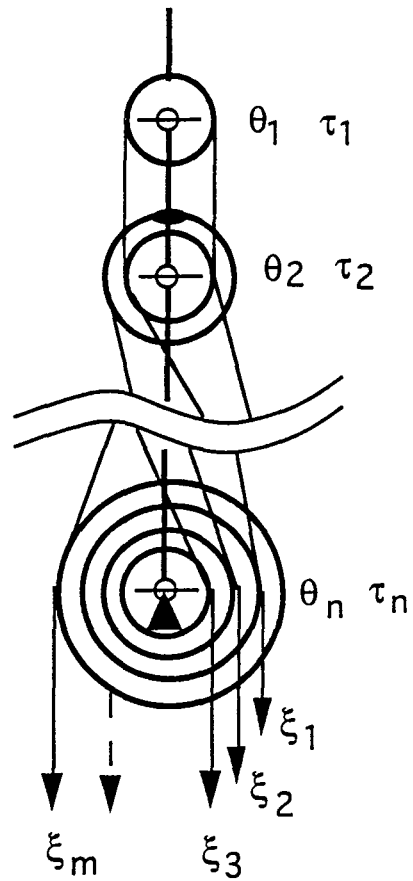


Figure 1: Planar schematic of an n -dof manipulator with m tendons

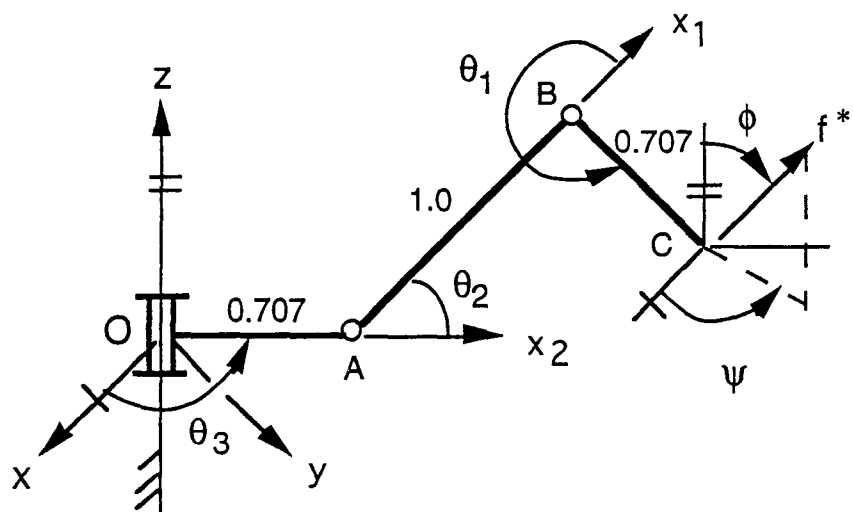


Figure 2: A three-dof spatial manipulator

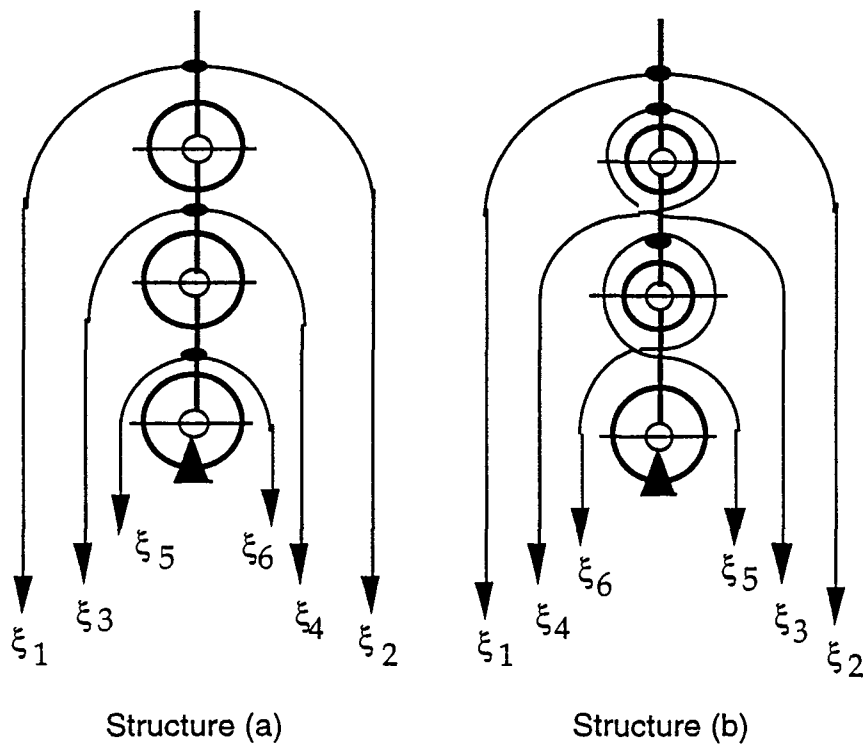


Figure 3: Tendon routings for transmission structures (a) and (b)

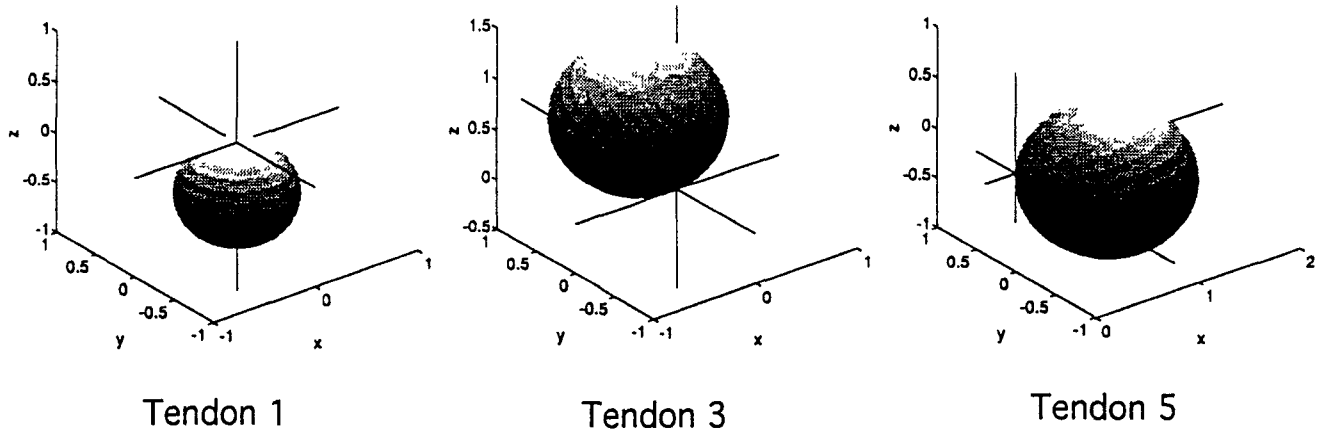


Figure 4: Spherical plots of tendon forces versus direction of applied force for structure (a)

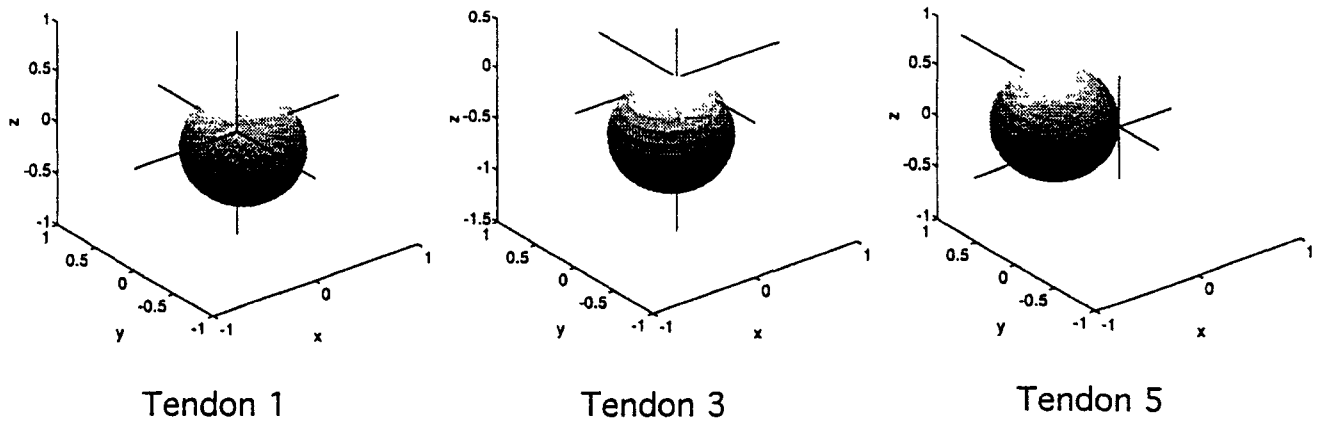


Figure 5: Spherical plots of tendon force versus direction of applied force for structure (b)